VOL. 17, NO. 14, JULY 2022 ISSN 1819-6608
ARPN Journal of Engineering and Applied Sciences

www.arpnjournals.com

TEMPERATURE CONTROL OF EXOTHERMIC POLYMERIZATION REACTION OF STYRENE INSIDE A CONTINUOUS STIRRED TANK REACTOR (CSTR)

Alvaro Realpe Jiménez, Karina Ballesteros Arrieta and María T. Acevedo Morantes
Department of Chemical Engineering, Research Group of Modeling of Particles and Processes, University of Cartagena, Campus Piedra Bolívar, Cartagena, Colombia
E-Mail: arealpe@unicartagena.edu.co

ABSTRACT

The main objective of this project is to control the temperature of styrene reaction inside jacket reactor by manipulating refrigerant flow of jacketfor the learning process of the process control course. Mathematical modelling inside the reactor and the jacket was carried out through moles and energy balances. The temperature control system was implemented using pneumatic valve, sensor-transmitter and dynamic simulation using SIMULINK. The proportional-integral controller reached steady state in a low time and the reaction temperature error was lower than that reached by the proportional controller. Also, the proportional-integral controller reacted fast to the step change in the set point of reaction temperature with a good performance. Likewise, the proportional-integral controller performed very well against a step change in the inlet temperature of polymer.

Keywords: temperature control, mathematical model, tuning, polymerization reaction.

1. INTRODUCTION

An automatic control system of the polymerization reaction improves product quality, maintain safety, and reduce production costs [1]. In addition, the quality of the products helps to increase the number of clients of the companies. Different types of reactors are used for continuous bulk styrene polymerization such as cooling reactor [2]. Modeling, simulation and control of continuous stirred tank Reactor (CSTR) with Cooling Jacket with high exothermic polymerization reactions are necessary for security, product quality and energy saving [3]. The properties of the styrene polymer are generally determined by average molecular weights and viscosity, which depends on the reaction temperature. Therefore, it is important to control the polymerization temperature, a key issue for the desirable properties of the polymer [4-7]. Controlling the chemical reaction occurring in a reactor requires engineers with complex knowledge on chemical process, control logical and instrumentation. Therefore, it is important to apply learning strategies to verify the theoretical knowledge explained to students in the classroom. Among the most used strategies to acquire skills in the area of process control are practices in the equipment in pilot scale to control variables such as level and temperature, and the other is the simulation of processes when there is no physical laboratory.

Temperature control of a jacketed reactor requires adjustment of the controller parameters. There are many tuning method for PID controller based on based on Lyapunov approach [8-9]. The performance of the parameters is safely analyzed in the temperature control simulation before implementing in the real process to avoid risk of explosion and low product quality [10]. The aim of this work is to control the temperature inside reactor vessel by manipulating the coolant flow inside jacket by using a pneumatic valve. Initially, mathematical modeling of the reaction process, valve, and sensor-transmitter were carried out. After, fitting of controller parameters, and finally simulation of the control loop using SIMULINK.

2. DESCRIPTION OF CHEMICAL PROCESS

The exothermic chemical reaction to be controlled is the polymerization of styrene in a jacketed CSTR. The general reaction that describes the polymerization of styrene is represented by Figure-1.

Figure-2 shows a jacketed reactor schematic diagram. The styrene enters the reactor with a variable flow and constant concentration. The polymerization reaction to produce polystyrene is exothermic, which is cooled with water passing through a jacket. The parameters of the reactor and the polymerization reaction are shown in Table-1.

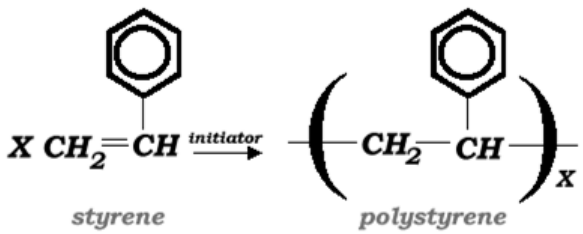

Figure-1. Chemical reaction of polymerization of styrene.

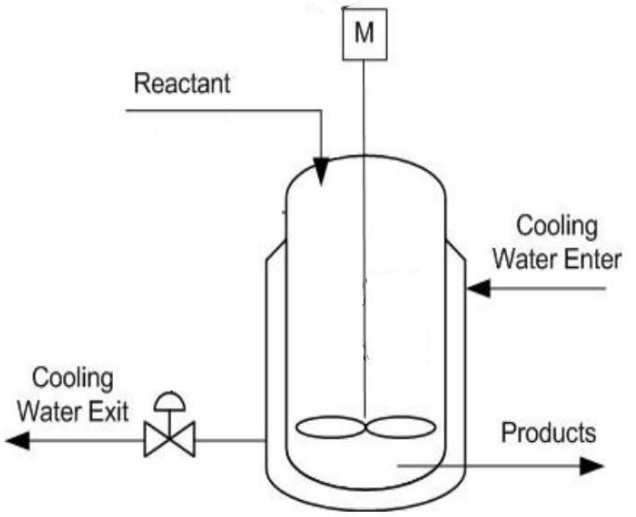

Figure-2. Continuous Stirred Tank Reactor (CSTR) with cooling jacket.

Table-1. Parameters of the polymerization reaction and the reactor.

$k_0 = 5.95 \times 10^{13} l \cdot s^{-1} \cdot mol^{-1}$	**Polymerization rate constant (frequency of collisions)**
$E = 124762.342 J \cdot mol^{-1}$	Activation energy of polymerization
$-\Delta H_r = 70020.34 J \cdot mol^{-1}$	Heat of reaction
$UA = 293.076 J \cdot s^{-1} K^{-1}$	Transfer area and the overall heat transfer coefficient
$\rho C_p = 1497.365 J \cdot l^{-1} K^{-1}$	heat capacity and density of reactants
$\rho_c C_{pc} = 3998.7048 J \cdot l^{-1} K^{-1}$	heat capacity and density of the refrigerant
$f_A = 0.098 l \cdot s^{-1}$	Monomer flow
$f_c = 0.129 l \cdot s^{-1}$	Cooling flow inside jacket
$V = 2500 l$	Reactor volume
$V_c = 35.124 l$	Jacket volume
$C_{Ai} = 8.6981 mol \cdot l^{-1}$	Inlet styrene concentration
$C_A = 1.7396 mol \cdot l^{-1}$	Styrene concentration at steady state inside the reactor
T_i= 330 K	Styrene temperature at the reactor inlet
T_{Ci}=295K	Coolant temperature at the jacket inlet
T=423K	Steady state temperature inside the reactor
T_C=340K	Steady state temperature in jacket

2.1 Mathematical Model of Continuous Stirred Tank Reactor (CSTR) with Cooling Jacket

Mass balance for styrene (component A) is given by equation 1:

$$f(t)C_{Ai}(t) - f(t)C_A(t) - Vr_A(t) = V\frac{dC_A(t)}{dt} \quad (1)$$

where C_{Ai} is the styrene concentration at the reactor inlet, C_A is the styrene concentration at the reactor outlet, f is volumetric flow of inlet and outlet of reactor, V is the rector volume and r_A is the reaction velocity for the polymerization reaction (equation 2).

$$r_A = k_0 e^{\frac{-E}{RT(t)}} C_A^2(t) \quad (2)$$

where $k_0$is the rate constant (frequency of collisions), T is the reaction temperature and E is the activation energy.

Energy balance for reaction inside reactor is given by equation 3.

$$f(t)\rho C_p T_i(t) - Vr_A(t)(\Delta H_r) - UA[T(t) - T_c(t)] - f(t)\rho C_p T(t) V\rho C_V \frac{dT(t)}{dt} \quad (3)$$

where $C_p$is the heat capacity at constant pressure, $C_V$is the heat capacity at constant volume, ΔH_r is reaction enthalpy, ρ is the density of mixture inside reactor, T_i is the styrene inlet temperature, T_c is the coolant temperature and A is the transfer area of heat.

Energy balance for coolant (C) inside jacket is given by equation 4.

$$f_C(t)\rho_C C_{PC} T_{Ci}(t) + UA[T(t) - T_C(t)] - f_C(t)\rho_C C_{PC} T_C(t) V_C \rho C_{VC} \frac{dT_C(t)}{dt} \quad (4)$$

where $C_{PC}$is the heat capacity at constant pressure of coolant, C_{VC} is the heat capacity at constant volume of coolant, ρ is the density of mixture inside reactor and T_i is the styrene inlet temperature.

The nonlinear terms of equations 1, 2, 3 and 4 are linearized using Taylor series as detailed below.

The nonlinear terms of mass balance for styrene (component A).

$$f(t)C_{Ai}(t) = \bar{f}\bar{C}_{Ai} + \bar{f}[C_{Ai}(t) - \bar{C}_{Ai}] + \bar{C}_A[f(t) - \bar{f}] \quad (5)$$

$$f(t)C_A(t) = \bar{f}\bar{C}_A + \bar{f}[C_A(t) - \bar{C}_A] + \bar{C}_A[f(t) - \bar{f}] \quad (6)$$

$$r_A(t) = k_0 e^{\frac{-E}{RT(t)}} C_A^2(t) = k_0 e^{\frac{-E}{R\bar{T}}} \bar{C}_A^2 + 2k_0 e^{\frac{-E}{R\bar{T}}} \bar{C}_A[C_A(t) - \bar{C}_A] + \bar{C}_A^2 \frac{E}{R\bar{T}^2} k_0 e^{\frac{-E}{R\bar{T}}}[T(t) - \bar{T}] \quad (7)$$

The nonlinear terms of energy balance for reaction inside reactor are:

$$f(t)T_i(t) = \bar{f}\bar{T}_i + \bar{f}[T_i(t) - T_i(t)] + \bar{T}_i[f(t) - \bar{f}] \quad (8)$$

$$f(t)T(t) = \bar{f}\bar{T} + \bar{f}[T(t) - T(t)] + \bar{T}[f(t) - \bar{f}] \quad (9)$$

The nonlinear terms of energy balance for coolant inside jacket

$$f_C(t)T_{Ci}(t) = \bar{f}_C\ \bar{T}_{Ci} + \bar{f}_C[T_{Ci}(t) - T_{Ci}(t)] + \bar{T}_{Ci}[f_C(t) - \bar{f}_C] \quad (10)$$

$$f_C(t)T_C(t) = \bar{f}_C\bar{T}_C + \bar{f}_C[T_C(t) - T_C(t)] + \bar{T}_C\ \ [f_C(t) - \bar{f}_C] \quad (11)$$

The linearized equations 5, 6 and 7 are replaced in equation 1, then equation is placed in terms of deviation variables and the Laplace transform is applied, obtaining the transfer function (equation 12).

$$C'_A(s) = \frac{K_1}{1+\tau S}C'_{Ai}(s) + \frac{K_2}{1+\tau S}f'(s) - \frac{K_3}{1+\tau S}T'(s) \quad (12)$$

where

$$\tau = \frac{V}{\bar{f} + 2Vk_0e^{\frac{-E}{R\bar{T}}}\bar{C}_A}$$

$$K_1 = \frac{\bar{f}}{\bar{f} + 2Vk_0e^{\frac{-E}{R\bar{T}}}\bar{C}_A}$$

$$K_2 = \frac{\overline{C}_{Ai} - \overline{C}_A}{\bar{f} + 2Vk_0e^{\frac{-E}{R\bar{T}}}\overline{C}_A}$$

$$K_3 = \frac{V\frac{E}{R\bar{T}^2}r_A}{\bar{f} + 2Vk_0e^{\frac{-E}{R\bar{T}}}\bar{C}_A}$$

The linearized equations 7, 8 and 9 are replaced in equation 3, then the equation is placed in terms of deviation variables and the Laplace transform is applied, obtaining the transfer function (equation 13).

$$T'(s) = \frac{K_4}{1+\tau_2 S}T'_i(s)\ + \frac{K_5}{1+\tau_2 S}f'(s) - \frac{K_6}{1+\tau_2 S}C'_A(s) + \frac{K_7}{1+\tau_2 S}T'_C(t) \quad (13)$$

where

$$K_4 = \frac{V\rho C_V}{V(\Delta H_r)\frac{E}{R\bar{T}^2}r_A + UA + \rho C_P\bar{f}}$$

$$K_4 = \frac{\rho C_p\bar{f}T'_i(s)}{V(\Delta H_r)\frac{E}{R\bar{T}^2}r_A + UA + \rho C_P\bar{f}}$$

$$K_5 = \frac{\rho C_P(\bar{T}_i - \bar{T})}{V(\Delta H_r)\frac{E}{R\bar{T}^2}r_A + UA + \rho C_P\bar{f}}$$

$$K_6 = \frac{2V(\Delta H_r)r_A}{V(\Delta H_r)\frac{E}{R\bar{T}^2}r_A + UA + \rho C_P\bar{f}}$$

$$K_6 = \frac{UA}{V(\Delta H_r)\frac{E}{R\bar{T}^2}r_A + UA + \rho C_P\bar{f}}$$

The linearized equations 10 and 11 are replaced in equation 4 then equation is placed in terms of deviation variables and the Laplace transform is applied, obtaining the transfer function (equation 14).

$$\mathrm{T'_C(t)} = \frac{\mathrm{K_8}}{\tau_3 \mathrm{S}\ +1}\mathrm{T'_{Ci}(s)} + \frac{\mathrm{K_9}}{\tau_3 \mathrm{S}\ +1}\mathrm{f'_C(s)} + \frac{\mathrm{K_{10}}}{\tau_3 \mathrm{S}\ +1}\mathrm{T'(t)} \quad (14)$$

Where:

$$\tau_3 = \frac{V\rho C_V}{UA + \rho_C C_{PC}\bar{f}_C}$$

$$K_8 = \frac{\rho_C C_{PC}\bar{f}_C}{UA + \rho_C C_{PC}\bar{f}_C}$$

$$K_9 = \frac{\rho_C C_{PC}(\bar{T}_{Ci} - \bar{T}_C)}{UA + \rho_C C_{PC}\bar{f}_C}$$

$$K_{10} = \frac{UA}{UA + \rho_C C_{PC}\bar{f}_C}$$

Considering constant volume and density. The inlet and outlet flows will be equal and constant, it will also be taken into account that the inlet concentration is constant, however, the inlet temperature varies with time (disturbance). Using these assumptions, equations 12, 13 and 14 reduce to equations 15, 16 and 17, respectively:

$$C'_A(s) = -\frac{K_3}{1+\tau S}T'(s) \quad (15)$$

$$T'_C(t) = \frac{K_9}{\tau_3 S\ +1}f'_C(s) + \frac{K_{10}}{\tau_3 S\ +1}T'(s) \quad (16)$$

$$\mathrm{T'(s)} = \frac{\mathrm{K_4}}{1+\tau_2 \mathrm{S}}\mathrm{T'_i(s)}\ - \frac{\mathrm{K_6}}{1+\tau_2 \mathrm{S}}\mathrm{C'_A(s)} + \frac{\mathrm{K_7}}{1+\tau_2 \mathrm{S}}\mathrm{T'_C(t)} \quad (17)$$

Replacing equations (15) and (16) in equation (17), equation 18 is obtained, which represents the temperature inside the reactor (controlled variable) as a function of the coolant flow (manipulated variable) and the inlet temperature of the styrene (disturbance).

$$T'(s) = \frac{K_7K_9(\tau_1 S+1)}{[(\tau_2 S-1)(\tau_1 S+1) - K_6K_3](\tau_3 S\ +1) - K_7K_{10}(\tau_1 S+1)}f'_C(s) + \frac{K_4(\tau_1 S+1)(\tau_3 S\ +1)}{[(\tau_2 S-1)(\tau_1 S+1) - K_6K_3](\tau_3 S\ +1) - K_7K_{10}(\tau_1 S+1)}T'_i(s) \quad (18)$$

where

$$G_p = \frac{T'(s)}{f'_C(s)} = \frac{K_7K_9(\tau_1 S+1)}{[(\tau_2 S-1)(\tau_1 S+1) - K_6K_3](\tau_3 S\ +1) - K_7K_{10}(\tau_1 S+1)} \quad (19)$$

$$G_D = \frac{T'(s)}{T'_i(s)} = \frac{K_4(\tau_1 S+1)(\tau_3 S\ +1)}{[(\tau_2 S-1)(\tau_1 S+1) - K_6K_3](\tau_3 S\ +1) - K_7K_{10}(\tau_1 S+1)} \quad (20)$$

2.2 Design of Sensor-Transmitter

A thermocouple (EFECTOR600® - TA3231) was used to monitor the temperature in the reactor, which is recommended for use in industrial processes for its resistance to corrosion. Through information on the operating range and time constant found in the technical sheet, the transfer function for the sensor was represented by a first order function (equation 21).

$$G_T(s) = \frac{K_T}{\tau_T\, s+1} \tag{21}$$

whereK_T is the sensor gain and τ_T is the time constant. The sensor gain is calculated using equation 22, which corresponds to the changes in the output variable between the changes in the input variable. The sensor output signal has a measurement range of -10 °C to 150 °C.

$$K_T = \frac{(20-4)\, mA}{150°C-(-10°C)} = 0.1\,\frac{mA}{°C} \tag{22}$$

The time constant of the transmitter is 0.65 min and replacing this in equation 21, the following transfer function for the transmitter is obtained (equation 23).

$$G_T(s) = \frac{0.1}{0.65\, s+1} \tag{23}$$

2.3 Design of Pneumatic Control Valve

The control valve will act on the flow of refrigerant circulating through the cooling jacket. A valve of equal percentage characteristics with a range ability parameter (α) of 50 was selected, which produces a very small change in flow at the beginning of the valve position displacement, but as it opens to the maximum opening position, the flow increases considerably. The valve is to be designed for 100% overcapacity and pressure drop can be considered constant. The valve selected to regulate the refrigerant flow in the jacket is BELIMO B2 series (LRB24-3), two-way. The model LRB24-3 has a time constant of 0.93 min and its transfer function is given by the equation 24.

$$G_v(s) = \frac{F_j(s)}{M(s)} = \frac{K_v}{\tau_v\, s+1}$$
$$G_v(s) = \frac{0.87}{7.3\, s+1} \tag{24}$$

3. RESULTS AND DISCUSSIONS

A feedback control system (Figure-3) consisting of a sensor-transmitter (equation 23), a pneumatic valve (equation 24), and a feedback controller is installed on the jacketed reactor represented by equation 18. The feedback control loop is represented by a block diagram as indicated in Figure-4.

Tuning of the parameters (K_c, y τ_I) of the feedback controller was performed using the closed loop method proposed by Ziegler and Nichols [11]. Based on the fine-tuning of the feedback controller parameters, different simulations were carried out using the SIMULINK software. Figure-5 shows simulations of feedback temperature control of a jacketed reactor using proportional controller at different proportional gain values. In this case, without disturbances for all simulations and the set point value was 250 °C. It is observed that the difference between the steady state and the desired value (error) decreases as the value of the proportional gain increases, the same behavior happens over time to reach the steady state. Meanwhile, the number of oscillations and their overshoot increase as the value of the proportional gain increases. These results are in accordance with the process control theory [12-13] and obtained by Realpe *et al*. [14].

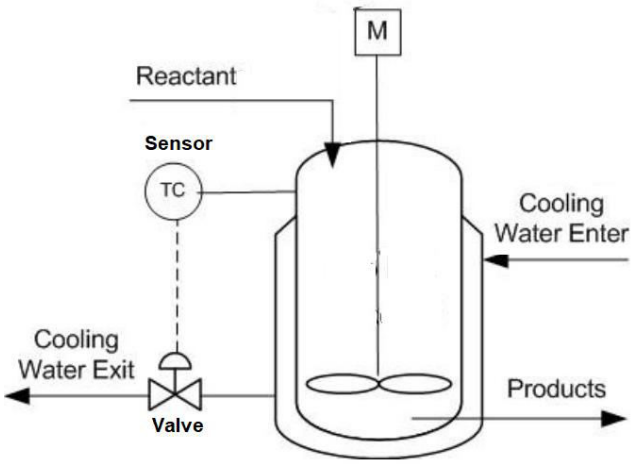

Figure-3. Feedback control system for Continuous Stirred Tank Reactor (CSTR) with cooling jacket.

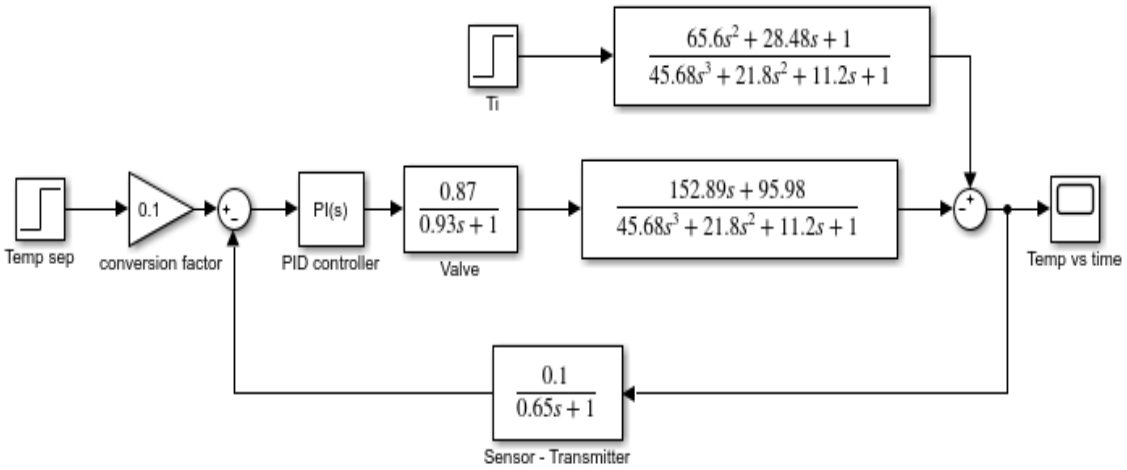

Figure-4. Closed-loop block diagram of a feedback control system.

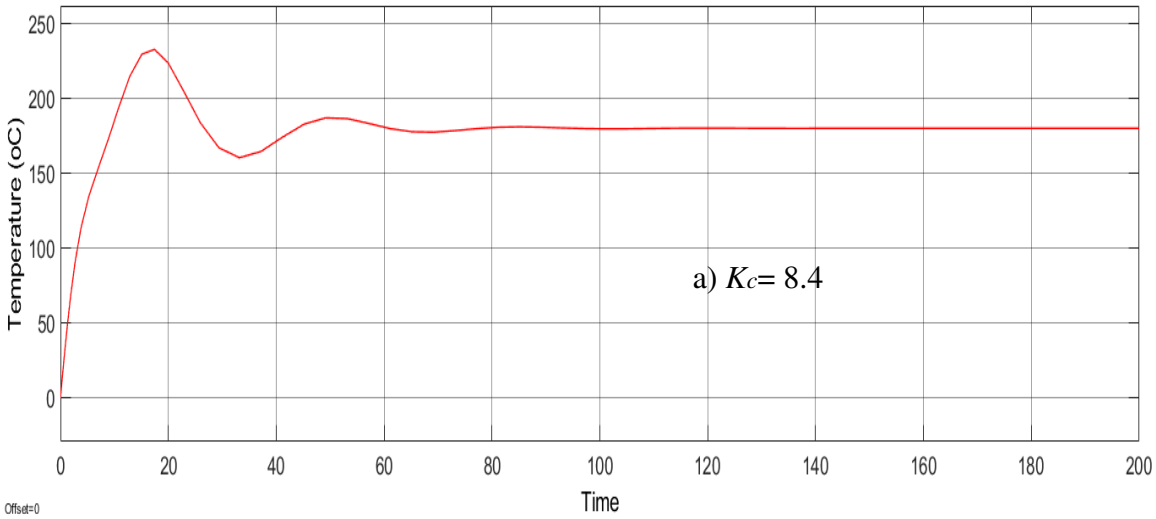

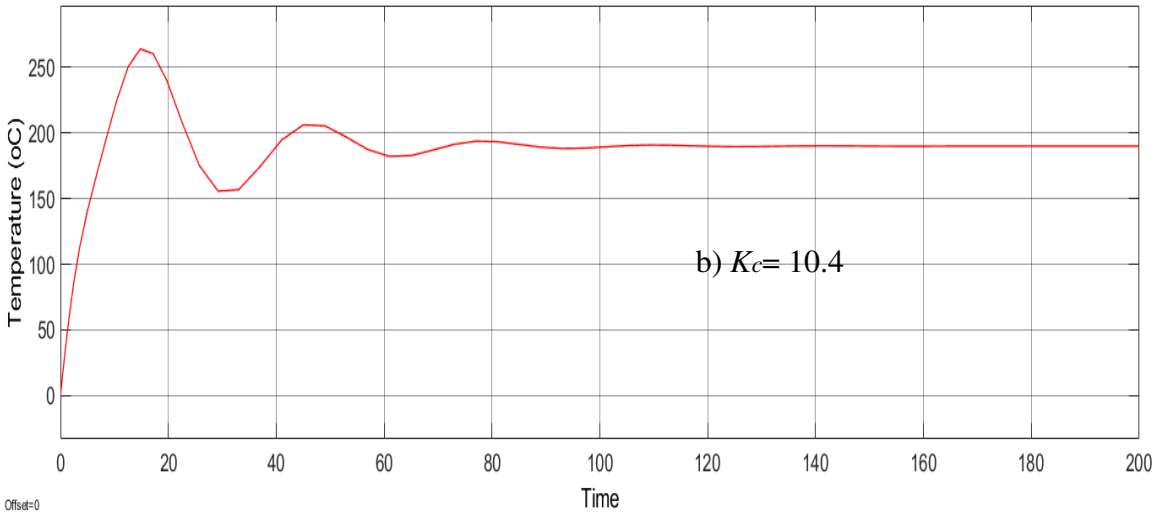

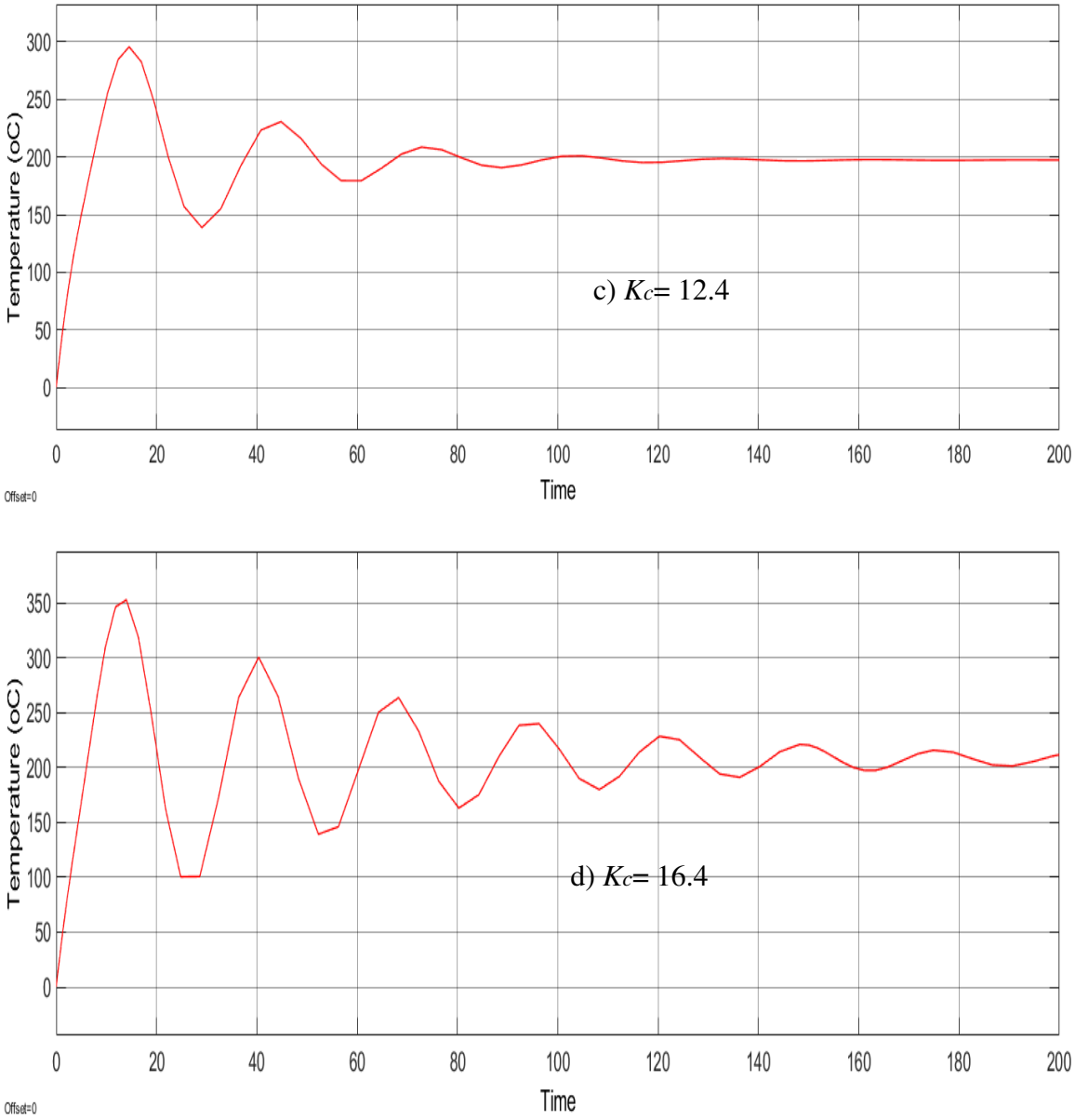

Figure-5. Simulations of feedback temperature control of a jacketed reactor using proportional controller (P) with set point value of 250 °C at a) *Kc*=8.4, b) *Kc*=10.4, *Kc*=12.4 and *Kc*=16.4

Figure-6 shows the effect of the step change of set point from 250 to 350 at minute 120 using proportional (P) controller. The controller acts fast before change in the set point, however, the set point is not reached. A similar behavior of the P controller is observed in Figure-7 when there is a step change of the inlet temperature (*Ti*) of styrene from 28 to 45 °C.

Therefore, the proportional-integral (PI) controller was implemented and fitted by closed loop method of Ziegler and Nichols. Figure-8 shows simulation of proportional-integral controller (PI) where the step changes of set point from 250 to 350 at 120 minutes is applied. It is observed the PI controller reached the set point faster than P controller, and the error of PI controller is lower than P controller. Meanwhile, the oscillations and overshoot of PI controller are lower than P controller. Similarly, Figure-9 shows the effect of the step change of input temperature (Ti) of styrene from 28 to 45°Cat 120 minutes using PI controller, showing a little peak up that drop to set point, indicating a good performance of PI controller.

The PID controller was tuned similarly to the PI controller using the Ziegler and Nichols closed loop method, however, the dynamic response of the reactor temperature was slower to reach steady state than the proportional controller as shown in Figure-10.

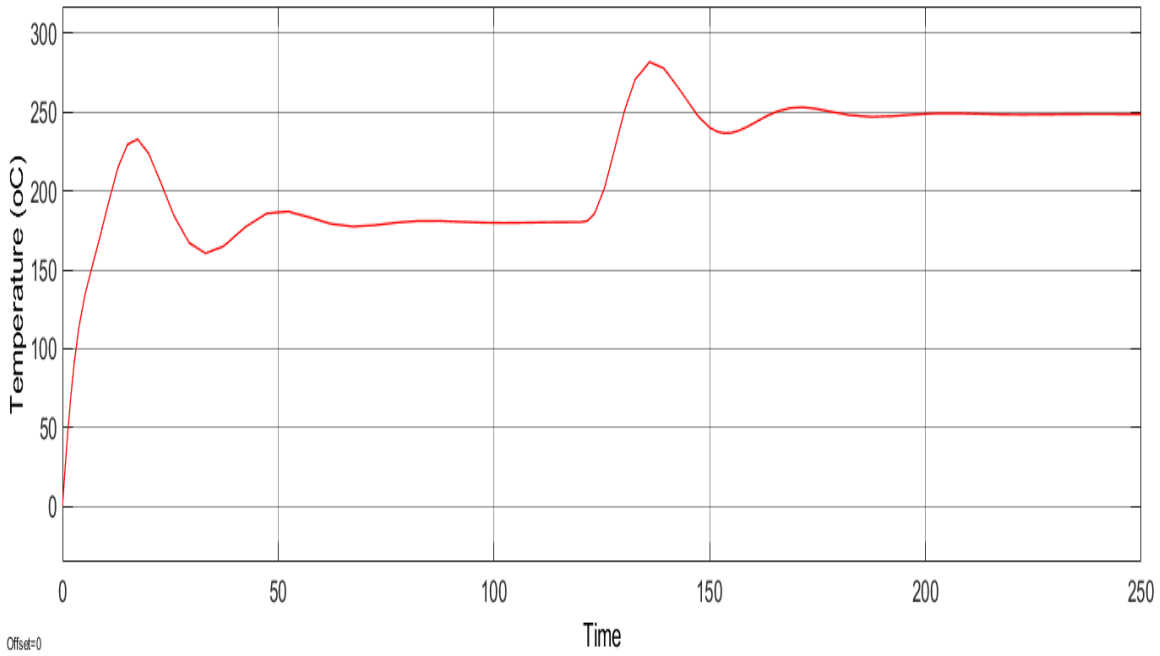

Figure-6. Effect of the step change of set point from 250 to 350°C at 120 minutes using proportional controller.

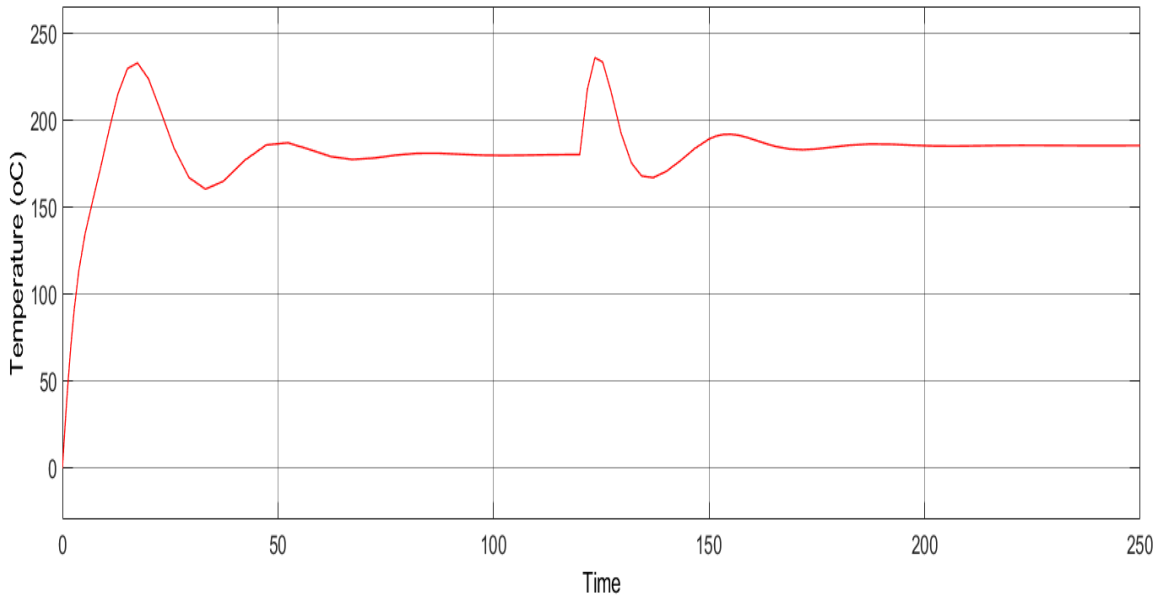

Figure-7. Effect of the step change of inlet temperature (*Ti*) of styrene from 28 to 45 °C at 120 minutes using proportional controller (P) with set point value of 250 °C.

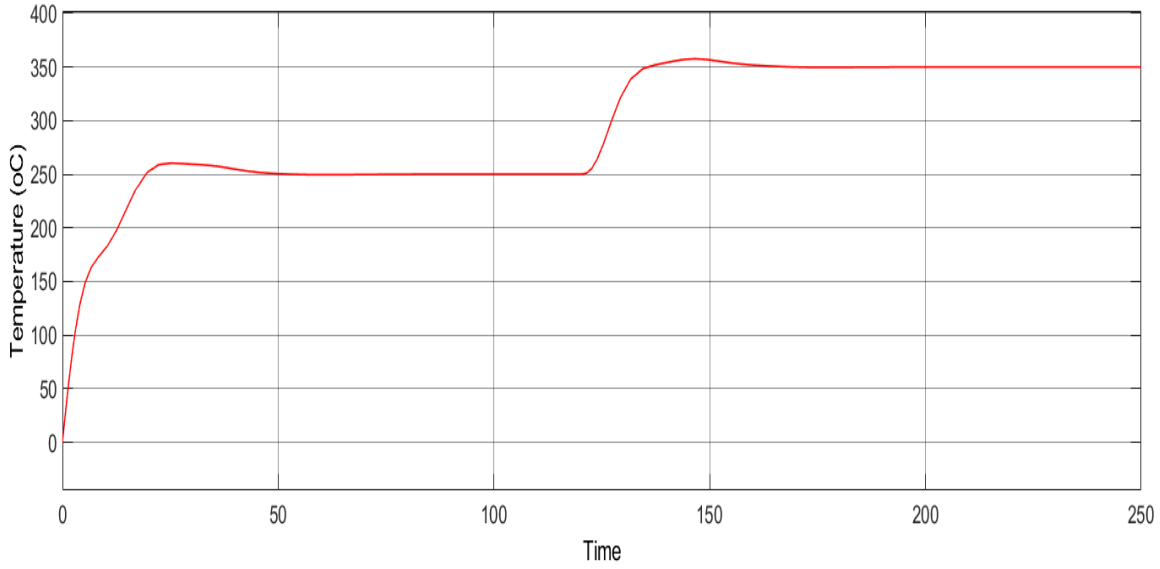

Figure-8. Effect of the step change of set point from 250 to 350 at 120 minutes using proportional-integral controller (PI) with set point value of 250 °C.

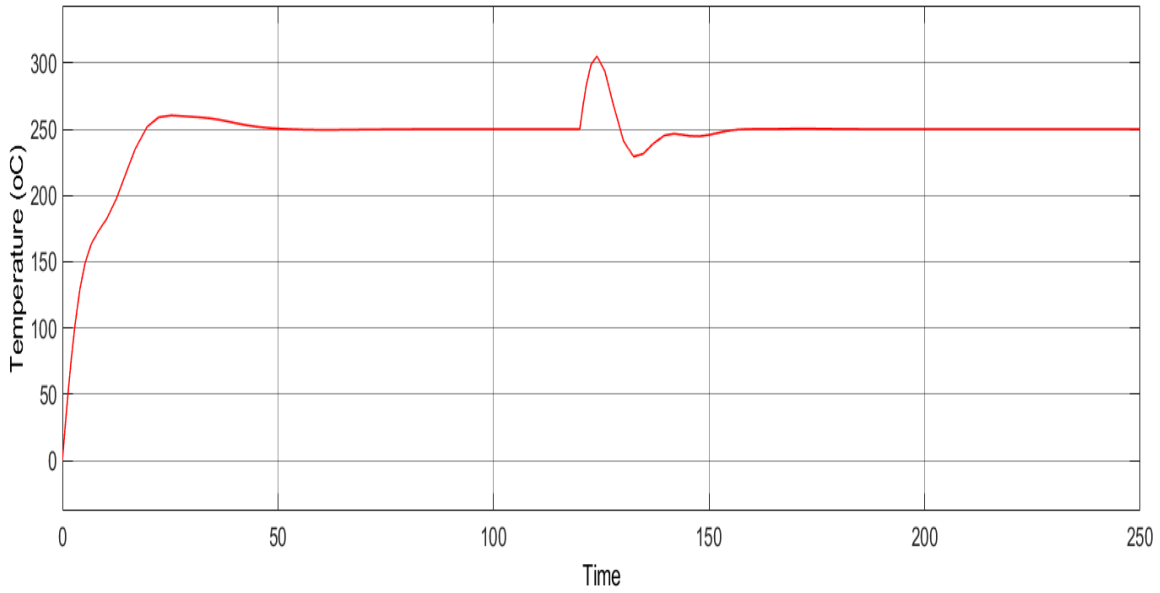

Figure-9. Effect of the step change of inlet temperature (Ti) of styrene from 28 to 45 °C at 120 minutes using proportional-integral controller (PI) with set point value of 250 °C.

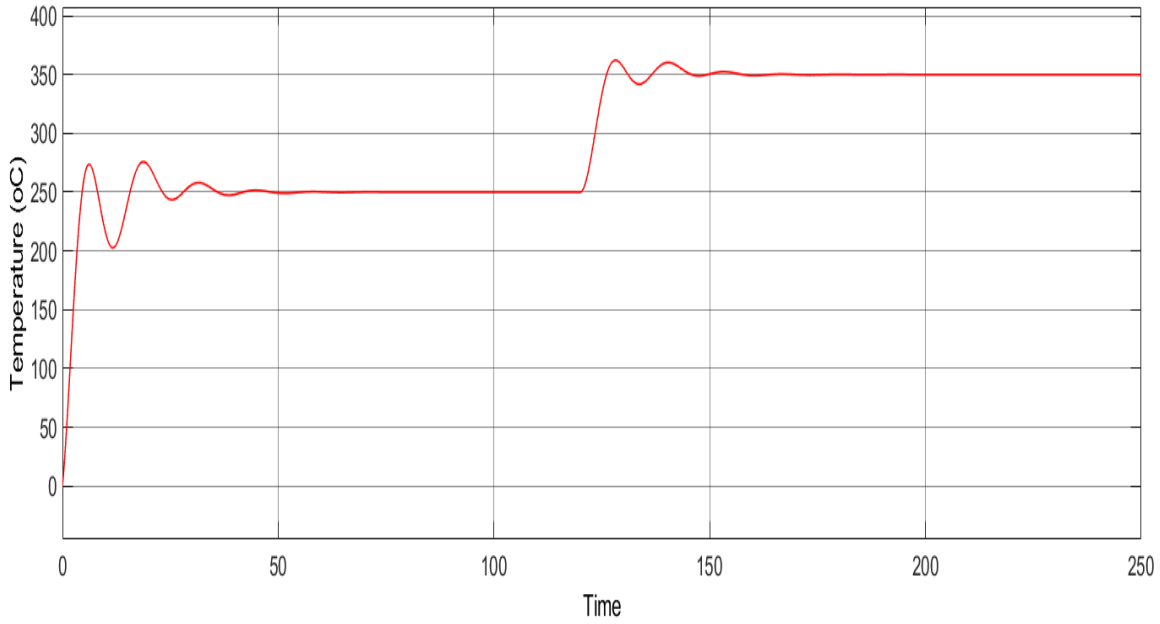

Figure-10. Effect of the step change of set point from 250 to 350 at 120 minutes using proportional-integral-derivative controller (PID) with set point value of 250 °C

4. CONCLUSIONS

The temperature control of the styrene polymerization reaction inside jacketed reactor was simulated using SIMULINK software. Initially, energy and mole balances were carried out within the reactor and the jacket, then the mathematical modelling of valve and sensor-transmitter were carried out. Proportional and proportional-integral controllers were tested, and PI controller reached a steady state faster than proportional controller. Furthermore, step changes in the set point and inlet temperature did not affect the performance of PI controller.

ACKNOWLEDGMENTS

Authors of this paper would like to express their gratitude to University of Cartagena for providing the recourses (Resolution No. 049-2019).

REFERENCES

[1] Caraballo V., R. Herrera and X. Sierra. 2010. Modelado Simulación y Control Automático de Evaporación en el proceso de Producción de la empresa Prolecta Ltda, Trabajo de Grado, Universidad de Cartagena, Cartagena.

[2] Chen C. C. 1994. A continuous bulk polymerization process for crystal polystyrene. Polym. Plast. Technol. Eng. 33, 55-58.

[3] Henderson L. S., Cornejo R. A. 1989. Temperature control of continuous, bulk styrene polymerization reactors and the influence of viscosity: an analytical study. Ind. Chem. Res. 28, 1644-1653.

[4] Vasco de Toledo, E. C., Martini, C. R. F., Maciel, M. R. W., Filho R. M. 2005. Process intensification for high operational performance target: autorefrigerated CSTR polymerization reactor. Comput. Chem. Eng. 29, 1447-1455.

[5] Feinberg M, Hildebrandt D. 1997. Optimal reactor design from a geometric viewpoint - I. Universal properties of the attainable region. Chem Eng Sci. 52(10): 1637-65.

[6] Feinberg M. 2000. Optimal reactor design from a geometric viewpoint. Part II. Critical side stream reactors. Chem. Eng. Sci. 55(13): 2455-79.

[7] Feinberg M. 2000. Optimal reactor design from a geometric viewpoint - III. Critical CFSTRs. Chem. Eng Sci. 55(17): 3553-65.

[8] Chang W. D., R. C. Huang, J. G. Hesieh. 2002. Self-tuning PID control for a class of nonlinear systems based on Lyapunov approach, J. Process Control. 12(2): 233-242.

[9] Erdogan S., G. Ozkan, M. Alpbaz. 1998. Self-tuning control of batch polymer- ization reactor, J. Chem. Eng. Jpn. 31(2): 499-505.

[10] De Graaff E., W. Ravesteijn. 2001. Training complete engineers: global enterprise and engineering education, Eur. J. Eng. Education. 26(4): 419-427.

[11] J. Ziegler and N. Nichols. 1942. Optimum Settings for Automatic Controller, Trans. American Society of Mechanical Engineers. 64: 759-768.

[12] Smith C. A., A. B. Corripio. 2006. Principles and Practices of Automatic Process Control, 3rd Edition, Wiley, New York.

[13] Seborg D., T. Edgar, D. Mellichamp and F. Doyle. 2011. Process Dynamics and Control, 3rd Ed., John Wiley & Sons, Inc., New York.

[14] Realpe A., Acevedo M, Franco D. 2018. Level Control in a System of Tanks in Interacting Mode Using Xcos Software, Contemporary Engineering Sciences. 11(2): 63-70.